Water Research 95 (2016) 150–158

Contents lists available at ScienceDirect

Water Research

journal homepage: www.elsevier.com/locate/watres

A novel method developed for estimating mineralization efficiencies and its application in PC and PEC degradations of large molecule biological compounds with unknown chemical formula

Guiying Li [a, b], Xiaolu Liu [b, c], Taicheng An [a, c, *], Po Keung Wong [d], Huijun Zhao [b, **]

[a] Institute of Environmental Health and Pollution Control, School of Environmental Science and Engineering, Guangdong University of Technology, Guangzhou, 510006, China
[b] Centre for Clean Environment and Energy, Gold Coast Campus, Griffith University, Queensland, 4222, Australia
[c] State Key Laboratory of Organic Geochemistry, Guangzhou Institute of Geochemistry, Chinese Academy of Sciences, Guangzhou, 510640, China
[d] School of Life Sciences, The Chinese University of Hong Kong, Shatin, NT, Hong Kong SAR, China

ARTICLE INFO

Article history:
Received 12 January 2016
Received in revised form
28 February 2016
Accepted 29 February 2016
Available online 3 March 2016

Keywords:
Method developing
Large molecule biological compounds
Unknown chemical formula
PC and PEC mineralization

ABSTRACT

A new method to estimate the photocatalytic (PC) and photoelectrocatalytic (PEC) mineralization efficiencies of large molecule biological compounds with unknown chemical formula in water was firstly developed and experimentally validated. The method employed chemical oxidation under the standard dichromate chemical oxygen demand (COD) conditions to obtain Q_{COD} values of model compounds with unknown chemical formula. The measured Q_{COD} values were used as the reference to replace Q_{COD} values of model compounds for calculation of the mineralization efficiencies (in %) by assuming the obtained Q_{COD} values are the measure of the theoretical charge required for the complete mineralization of organic pollutants. Total organic carbon (TOC) was also employed as a reference to confirm the mineralization capacity of dichromate chemical oxidation. The developed method was applied to determine the degradation extent of model compounds, such as bovine serum albumin (BSA), lecithin and bacterial DNA, by PC and PEC. Incomplete PC mineralization of all large molecule biological compounds was observed, especially for BSA. But the introduction of electrochemical technique into a PC oxidation process could profoundly improve the mineralization efficiencies of model compounds. PEC mineralization efficiencies of bacterial DNA was the highest, while that of lecithin was the lowest. Overall, PEC degradation method was found to be much effective than PC method for all large molecule biological compounds investigated, with PEC/PC mineralization ratios followed an order of BSA > lecithin > DNA.

1. Introduction

During the past several decades, an elevated interest is observable in the oxidative damage of large molecule biological compounds, such as protein, DNA and lipid (Dalrymple et al., 2011; Kurz et al., 2011; Yin et al., 2011), since these biomolecules are the building blocks of the living microorganisms, and the accumulation of these pollutants can result in a number of detrimental effects on human being during the traditional water disinfection (Westgatet and Park, 2010; Chuang et al., 2013). For instance, protein contaminated water is very harmful due to their infection property because they can be either free or attached to microorganisms (Paspaltsis et al., 2009); Another large molecules biological compound, amino acids, the building block of protein, have been suggested as the likely precursors of carcinogenic nitrogenous disinfection byproducts upon reacting with chlorine or chloramines (Chuang et al., 2013; Bond et al., 2015). In addition, the antibiotic resistance genes are also a new kind of emerging contaminants in water environments, which has been a major driving force behind the evolution of multidrug resistant bacteria (Martinez, 2008). Therefore, much attention has been paid to the degradation and mineralization of large molecules biological compound in water environments.

* Corresponding author. Guangzhou Institute of Geochemistry, Chinese Academy of Sciences, Guangzhou, 510640, China.
** Corresponding author.
E-mail addresses: antc99@gdut.edu.cn, antc99@gig.ac.cn (T. An), h.zhao@griffith.edu.au (H. Zhao).

http://dx.doi.org/10.1016/j.watres.2016.02.066
0043-1354/

It is well known that various techniques can be employed to oxidize these large molecules biological compound early (Sharma et al., 2011; Zeleny et al., 2012; Cadet and Wagner, 2013; Nowicka et al., 2013). However, the currently most employed quantification method used their initial and final mass concentrations to calculate the degradation or mineralization extent of the target biological compounds (Ji et al., 2014; Wang et al., 2014; Xu et al., 2014). These methods using mass concentration just estimate the mineralization extent without consideration of chemical structures difference of various organics.

Recently, a unique rapid methodology (PECOD) was developed by us to determine the degradation extent of dissolved organics in a water with directly quantifying the extent of electron (e^-) transfer onto a TiO_2 nanoporous film electrode with an exhaustive photoelectrocatalytic (PEC) degradation of organics process (Zhao et al., 2004, 2007). This is because the different oxidation degrees of same organic compound require different transferring numbers of e^- (Zhao et al., 2007; Li et al., 2013b). The use of e^- transfer to quantify the organics degradation extent allows a more meaningful comparison of organics with different chemical structures with e^- transfer numbers, due to such a non-characteristic unit represents the e^- demands for the complete mineralization, regardless of their mass concentration. Nevertheless, this method can only be used to estimate the degradation extent of organics with known chemical formula. For example, the complete mineralization of many small biomolecules like nucleotides (Li et al., 2013b), nucleotide bases (Li et al., 2015b) and amino acids (Li et al., 2015a) have already been investigated in detail by us. However, compared with the small molecule biological compounds, the quantification of the mineralization/degradation extent of large molecules biological compound without chemical formula such as proteins, DNA and lipids are more complex and very difficult at present stage. One of the most important difficulties is that the precise chemical formula of these numerous large molecule biological compounds are unknown. Thus, this means that the method developed previously cannot be properly used to investigate the mineralization of these large molecules biological compound due to that the theoretical charge required to mineralize these large biological compounds cannot be calculated without their chemical formula.

In addition, as aforementioned, large molecule biological compounds are the building blocks of microorganisms for example bacteria and virus. The conventional biohazards inactivation efficiency usually evaluated by the standard plate count method only to estimate the cell viabilities before and after various disinfection treatments (Li et al., 2011, 2013a; Nie et al., 2014; Tobaldi et al., 2014). However, the decomposition products of the incomplete-mineralized components including various levels building blocks are highly complex associated with various biological array during these disinfection processes (Li et al., 2014; Sun et al., 2014). Thus, the quantification of the mineralization extent of the biohazards can be examined by total organic carbon (TOC), but it is very difficult to build any relationship of the mineralization efficiencies with the e^- transfer during the PC and PEC inactivation of biohazards.

Thus, to overcome this difficulty, in this study, a new method was firstly developed to estimate the photocatalytic (PC) and photoelectrocatalytic (PEC) mineralization efficiencies of large molecule biological compounds with unknown chemical formula in water, and subsequently used to experimentally validate the mineralization of the PC and PEC degradation of representative building blocks of microorganisms, the large molecules biological compounds, such as proteins, DNA and lipids. This built method will provide an effective means to simply evaluate the degradation and damage of these building blocks of biohazards as well as their degradation products, which will be, in turn, offer us a quantitative method to understand the killing mechanism of bacteria and viruses as the damage was imposed on these building blocks.

2. Experimental section

2.1. Materials

Indium tin oxide conducting glass slides (ITO, 8 Ω/square) were purchased from Delta Technologies Ltd. (USA). Titanium butoxide (97%, Aldrich), sucrose (AR grade, UNIVAR), BSA (>98%, Biotech), and L-α-lecithin (99%, Sigma) were used as received. Other chemicals used were of analytical grade and purchased from Sigma unless otherwise stated. Genomic DNA of *Escherichia coli* is extracted according to the reference (Sambrook et al., 1989). All solutions were prepared using high purity deionized water (Millipore Corp., 18 M Ω cm).

2.2. Apparatus and methods

Both PC and PEC degradation experiments were performed under identical UV intensity using the same UV-LED/TiO_2 photoelectrochemical cell in Fig. S1 as Supporting information. The cell consists of a TiO_2 photoanode as the working electrode, an Ag/AgCl reference electrode and a Pt mesh auxiliary electrode. The TiO_2 photoanode was prepared by hydrolysis of titanium butoxide according to the method described in our previous publication (Zhao et al., 2007). An UV-LED (NCCU033(T), Nichia Corporation) was used as the illumination source. The specified peak wavelength of the LED was 365 nm with a spectrum half width of 8 nm. The UV intensity was adjusted by a power supply and measured with an UV-irradiance meter (UV-A, Beijing Normal University). For PEC degradation experiments, a 2.0 M $NaNO_3$ solution was used as the supporting electrolyte. A voltammograph (cv-27, BAS) was used for electrochemical control. Potential and current signals were monitored using a Macintosh computer (7220/200) coupled with a Maclab 400 interface (AD Instruments). PC degradation experiments were conducted under identical experimental conditions as PEC experiments, except the electrochemical system was disconnected.

2.3. Standard chemical oxygen demand (COD) and total organic carbon (TOC) analyses

Standard COD value (dichromate method) of the samples was measured with an EPA approved COD analyzer (NOVA 30, Merck). Each COD value was the mean value of a triplicate measurement.

TOC content of samples was measured with TOC-V_{CPH}-V/TOC-V_{CPN} Total Organic Carbon Analyzer (Shimadzu Corporation, Japan). Standardization curves for the IC and TC determinations were prepared according to the manufacturer's instructions. Triplicate analyses were performed on each sample.

3. Results and discussion

3.1. Quantification principle

An oxidative mineralization process is essentially an e^- transfer process. Therefore, the ratio between the experimentally measured number of transferred e^- (Q_{exp}) during the degradation and the theoretically required number of transferred e^- (Q_{th}) for stoichiometric mineralization is the most simple and meaningful way of quantifying the percentage of mineralization (η). That is:

$$\eta = \frac{Q_{\exp}}{Q_{th}} \times 100\% \quad (1)$$

When the chemical formula of a compound is known, the number of the transferred e^- (n) can be obtained from the stoichiometric mineralization of reactants (Zhao et al., 2004; Zhang et al., 2006):

$$C_yH_mO_jN_kX_q + (2y - j)H_2O \rightarrow yCO_2 + qX^- + kNH_3 + (4y - 2j + m - 3k)H^+ + (4y - 2j + m - 3k - q)e^- \quad (2a)$$

$$n = 4y - 2j + m - 3k - q \quad (2b)$$

where N and X represents nitrogen and halogen atoms, respectively. The numbers of C, H, O, N and X atoms in the compound are represented by y, m, j, k and q, respectively. n refers to the number of transferred e^- for mineralization.

The Q_{th} of a compound with known chemical formula can then calculated based on Faraday's law:

$$Q_{th} = nFVC \quad (3)$$

where, F is the Faraday constant and V and C are the sample volume and concentration, respectively.

However, the precise chemical formulas of many complex large molecule biological compounds are unknown. Under this circumstance, if the degradation of a large molecule biological compound under the standard dichromate COD determination conditions can be regarded as 'stoichiometric mineralization', then the experimentally measured change transfer (Q_{COD}) from the determined COD value can be used to replace the Q_{th}. Considering that for COD calculation, one O_2 is equivalent to 4 transferred e^- (Zhao et al., 2004), the Q_{th} of large molecule biological compounds with unknown formula can therefore be expressed as:

$$Q_{th} = Q_{COD} = \frac{[\mathrm{COD\ (mg/LO_2)}]}{32000} \times 4FV \quad (4)$$

where, Q_{COD} is the equivalent charge obtained from the determined COD value. F is the Faraday constant; and V is the sample volume.

For PEC degradation, the Q_{exp} can be readily determined by measuring the net transferred charge (Q_{net}) originated from the oxidative degradation of large molecule biological compounds, as illustrated in Fig. S2 (Zhang et al., 2004). That is:

$$Q_{\exp} = Q_{net} = Q_{total} - Q_{blank} = \int i_{total}dt - \int i_{blank}dt \quad (5)$$

where, i_{total} is the total photocurrent resulting from photocatalytic oxidation of large molecule biological compound and water. i_{blank} is the photocurrent resulting essentially from photocatalytic oxidation of water in absence of large molecule biological compound.

Therefore, the percentage of PEC mineralization can be written as:

$$\eta_{PEC} = \frac{Q_{\exp}}{Q_{th}} \times 100\% = \frac{Q_{net}}{Q_{th}} \times 100\% \quad (6)$$

For PC degradation, the Q_{exp} can be simply determined by PEC method. In brief, the net transferred charges for the sample before (Q^1_{net}) and after (Q^2_{net}) PC degradation treatment can be photoelectrocatalytically determined as illustrated in Fig. S3. The Q_{exp} of PC degradation can be written as:

$$Q_{\exp} = Q^1_{net} - Q^2_{net} \quad (7)$$

where, $Q^1_{net} - Q^2_{net} = Q_{\Delta net}$

$$= \left(\int i_1 dt - \int i_{blank}dt\right) - \left(\int i_2 dt - \int i_{blank}dt\right) = \int i_1 dt - \int i_2 dt \quad (7a)$$

The percentage of PC mineralization (η_{PC}) can therefore be written as:

$$\eta_{PC} = \frac{Q_{\exp}}{Q_{th}} \times 100\% = \frac{Q^1_{net} - Q^2_{net}}{Q_{th}} \times 100\% \quad (8)$$

3.2. Calibration of equivalent electrons transferred for the mineralization of large molecule biological compounds with unknown chemical formula

From the Eqs. (3) and (4), we can obtain:

$$\mathrm{COD} = 8000\ nC \quad (9)$$

Eq. (9) can be used to directly quantify the n value of a sample when COD is obtained, since the C, the concentration, is known.

To determine whether the proposed method can be applied to determinate the mineralization percentage of organics, two sets of experiments were performed. Firstly, a pure organic compound with known chemical formula, for example sucrose was subjected to the examination. According to Eq. (9), the theoretical and experimental mole of e^- can be obtained from theoretical and experimental COD values. The relationship between the theoretical and experimental mole of e^- and the sucrose concentration is given in Fig. 1a.

Theoretically, the numbers of e^- required for the mineralization of 1 mol of sucrose ($C_{12}H_{22}O_{11}$) is n = 48 mol as described by Eq. (2b), which is the same value as slope obtained from the theoretical curve in Fig. 1a. Experimentally, the mole of e^- (data from standard COD results) obtained were directly proportional to the sucrose concentration with an experimental slope value of 48.108. Comparatively, two linear lines almost fit into one linear line. Considering the experimental errors and the purity of the reagent, the experimental slope value of the curve (48.108) was found to be almost the same as the slope value of the theoretical curve. These results demonstrated that sucrose can be stoichiometrically mineralized to CO_2, H_2O by a strong oxidizing agent (e.g., dichromate) under acidic condition. In other word, the Q_{COD} obtained using the standard COD method could be used to replace the Q_{th} to calculate the mineralization extent. This is because the same amount of e^- transferred to the chemical oxidizing agent during a chemical oxidation process. This is also because that the different oxidation degrees of same organics require transferring different numbers of e^- (Zhao et al., 2007).

To further validate the oxidation capability of standard COD to organic compound, TOC test, which uses heat, ultraviolet light, or a strong chemical oxidant (or a combination of the three) to completely oxidize organic compounds to CO_2 and H_2O, was also carried out simultaneously for sucrose analysis. TOC is correlated to COD for a given organic compound. For a given organics, the correlation between the theoretical COD and the theoretical TOC values (COD_{th}/TOC_{th}) should be a fixed value, if the stoichiometric

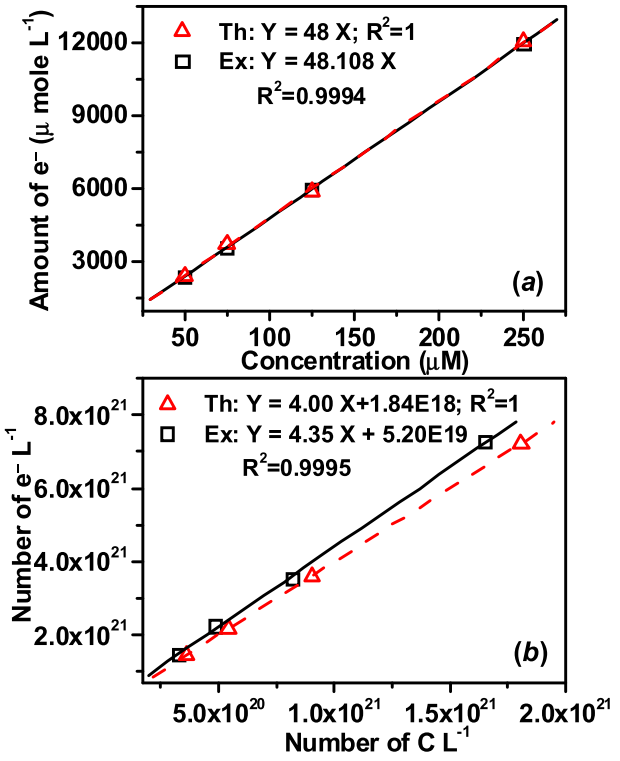

Fig. 1. Correlation between (a) the mole of electrons and the concentration of sucrose; (b) the number of electrons per liter and the number of carbons per liter of different concentration of sucrose (△: theoretical; □: experimental).

mineralization has been achieved during the chemical oxidation process. In other word, the chemical stoichiometric mineralization has been achieved when the ratio of experimental COD/experimental TOC (COD_{chem}/TOC_{exp}) is the same as the value of COD_{th}/TOC_{th}. The TOC and COD values can be readily converted as the number of carbons per liter and the number of e^- per liter, respectively. Fig. 1b shows the plot of the number of e^- per liter ($e^- L^{-1}$) against the number of carbons per liter ($C\ L^{-1}$) from both theoretical and experimental data. As shown, the linear relationships between the number of e^- per liter and the number of carbons per liter were obtained. Slopes of 4.00 and 4.35 $e^-\ C^{-1}$ were obtained for the theoretical and experimental data of sucrose, respectively. The experimental slope value was 108.8% of the theoretical slope value. Considering the analytical errors associated with both the COD_{chem} and TOC_{exp} measurements as well as these errors contribute to scatter on both axes, it is reasonable to claim that the analytical correlation factor of number of e^- per carbon ($e^- C^{-1}$) resulted from the experimental results are very close to the theoretical results. It is doubtless to say that the sucrose was totally oxidized. From studies such as these scheme, it was concluded that the COD_{chem}, which is also called standard COD (COD_{st}) values, can be used as a substitute for theoretical COD. Q_{COD} can be calculated according to the Eq. (4). Subsequently, the mineralization percentage of PEC and PC degradation of organics with known chemical formula can be achieved according to the Eqs. (6) and (8).

A second series of experiments was carried out using BSA as a model compound to represent the large molecules biological compound with unknown chemical formula to validate the developed method. Though exact chemical formula of BSA is unknown, BSA has been reported to consist of 607 amino acid residues (Table S1), 17 disulfide bonds and a molecular weight of ~69.4 kDa (Brown, 1975; Hirayama et al., 1990). Theoretically, according to the e^- transfer number for complete mineralization of all BSA residues, the numbers of e^- required for the mineralization of 1 mol of all the amino acids residues of BSA without disulfide bonds can be calculated as n = 13,040 mol (Table S1). However, the BSA molecule has 17 disulfide bonds. According to the following reaction:

$$2\ RSH \rightarrow RS - SR + 2H^+ + 2e^- \quad (10)$$

The numbers of e^- required for mineralization of 1 mol of BSA is n = 13,006 mol.

Similarly, the relationship between the theoretical and experimental mole of e^- and the BSA concentration is given in Fig. 2a. Linear increase for both the theoretical and experimental mole of e^- was observed with the increase of the BSA concentration. The slope value of the theoretical curve was found to be 13,006 μmole e^- per μmole of BSA, which represents the number of e^- required for mineralization of 1 mol of BSA. The slope of the experimental curve was found to be 12,495 μmole e^- per μmole of BSA, which is

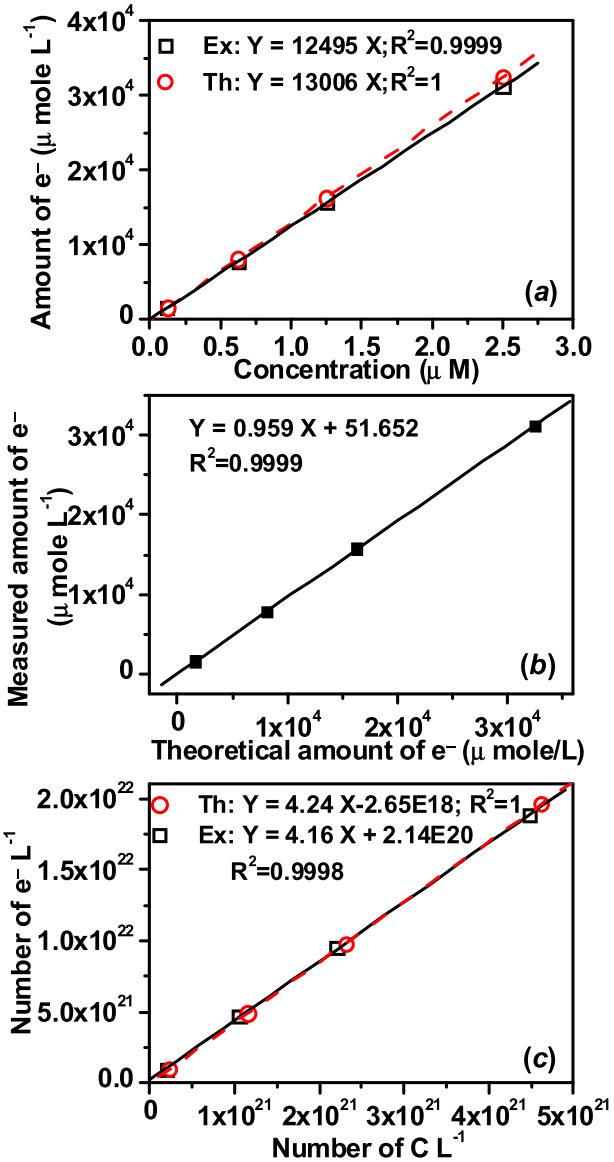

Fig. 2. Correlation between (a) the mole of electrons and the concentration of BSA (○: theoretical; □: experimental); (b) the measured amount of electrons and the theoretical amount of electrons with different concentration of BSA; and (c) the number of electrons per liter and the number of carbons per liter of different concentration of BSA (○: theoretical; □: experimental).

very close to the slope value of the theoretical curve. This can be further evidenced by plotting the measured amount of e^- against the theoretical amount of e^- values as shown in Fig. 2b, where the line of the best fit with the slope of 0.959 and $R^2 = 0.9999$ were obtained. This demonstrates that the method measures essentially the theoretical amount of e^- values. Considering the experimental errors and the purity of the reagent, it is reasonable to conclude that there is no essential difference between the theoretical and experimental results, and BSA can be fully mineralized by using standard COD method.

Fig. 2c shows the plot of the number of e^- per liter (e^- L^{-1}) against the number of carbons per liter (C L^{-1}) from both theoretical and experimental data. The linear relationships between the number of e^- per liter and the number of carbons per liter were achieved theoretically and experimentally. The slope values of 4.24 and 4.16 e^- C^{-1} were obtained for the theoretical and experimental data of BSA, respectively. The experimental slope value was 97.9% of the theoretical slope value. Considering that there are analytical errors associated with both the COD_{chem} and TOC_{exp} measurements and that these errors contribute to scatter on both axes, it is reasonable to claim that the analytical correlation factor of number of e^- per carbon (e^- C^{-1}) resulted from the experimental results are very close to theoretical values. It is doubtless that BSA was fully mineralized. Accordingly, we can conclude that the complete mineralization of BSA can be achieved via the chemical oxidation process under the standard COD determination conditions. The Q_{COD} calculated based on the measured COD values according to the Eq. (4) can therefore be use to replace Q_{th} in the mineralization percentages of PEC and PC degradation of organics with unknown chemical formula according to the Eqs. (6) and (8).

3.3. PC and PEC degradation of large molecule biological compounds with unknown chemical formula

3.3.1. PC and PEC degradation of BSA

PC and PEC degradation of BSA was firstly carried out. Fig. S4 shows a set of typical photocurrent–time profiles obtained from BSA samples before (original sample) and after PC treatment. These photocurrent profiles are used to obtain the net charges of the sample before and after PC degradation and calculated in accordance with Eq. (7a).

Fig. S5 shows a set of typical photocurrent–time profiles obtained from BSA samples (8–80 mg L^{-1}) during PEC treatment. These photocurrent profiles are used to obtain the net charges (Q_{net}) of the sample after PEC degradation and calculated in accordance with Eq. (5). The insert within Fig. S5 is the calibration curve of the responses under a constant applied potential bias (+0.30 V *vs.* Ag/AgCl) and light intensity (8.0 mW cm^{-2}).

With the blank solution (2.0 M $NaNO_3$), the photocurrent decreased rapidly and attained its steady-state within 50 s. The initial photocurrent spike was due to the PC oxidation of the adsorbed water accumulated at the electrode surface. While for the samples containing BSA, the initial photocurrent spikes were higher than that of the blank solution and increased steadily with the increase of BSA concentration. Within BSA concentrations investigated, for all cases, well-defined steady-state currents with designated reaction endpoint of the PC degradation of BSA were obtained. The endpoint herein refereed to the photocurrent of a BSA containing sample reaches the same value as the steady-state photocurrent of the blank solution. Within lower BSA concentration range (i.e., 8–40 mg L^{-1}), the photocurrents declined monotonically during the degradation process. Comparatively, the photocurrent of 80 mg L^{-1} BSA protruded at the beginning of the reaction and then declined subsequently. A possible reason for fluctuating photocurrent curve at the beginning part of the reaction could be due to the formation of stable intermediates and the accumulation of these intermediates at the electrode surface as a result of PC reaction. With the prolongation of the degradation reaction, these intermediates together with the BSA residue can be decomposed into smaller and less stable intermediates (Sun et al., 2014), which were clearly reflected by the subsequent photocurrent decrease and the attainment to the blank solution steady-state photocurrent level. It is worth noting that this phenomenon took place only when organics concentration is high, because the produced intermediates can be instantly decomposed at low concentration of organics degradation process due to the powerful photogenerated-hole oxidation capacity. It was also found that an increase in BSA concentration can lead to an increase in the integration of photocurrents (total amount of transferred charge during the degradation). The net charge increase was found to be directly proportional to BSA concentrations, as shown in the insert of Fig. S5, where a good linearity with a R^2 value of 0.9997 was obtained.

The applicability of the method developed in this study was then tested for determining the PC and PEC mineralization percentages of large molecule biological compounds with unknown chemical formulas. BSA was chosen as a model globular protein because of its physiological importance, easy separation and purification (Wang et al., 2009). Fig. 3a demonstrates the PC degradation percentages of BSA under the exhaustive condition in the thin-layer cell. The results show that PC mineralization of BSA was very difficult to be achieved. About 11.6% of 8 mg L^{-1} of BSA can be fully mineralized by converting the carbon atoms to CO_2, hydrogen to H_2O and nitrogen to NH_3. When the initial BSA concentrations were increased to 16 and 40 mg L^{-1}, only 0.6% and 0.4% of the BSA can be completely oxidized, respectively. The PC degradation was essentially stopped when the initial BSA concentration increased to 80 mg L^{-1}.

The reason for BSA hard to be PC degraded may be due to that BSA molecule is a huge polymeric amide (A–CONH–B), and a chain of amino acid "residues" linked by peptide bonds formed *via* the condensation of amino acids. The photocatalytically generated •OH on the TiO_2 particle surface is a powerful protein-modifying agent. The PC degradation can produce a great number of intermediates from 20 common side chains and the peptide backbone (Dean et al., 1997; Hawkins and Davies, 2001; Paspaltsis et al., 2009). Exposing to •OH, two types of damage to the protein molecules may occur. One is the fragmentation and another is aggregation (Bosshard et al., 2010; Sun et al., 2014). In this research, BSA might undergo progressive covalent cross-linking to form dimers, trimers and even tetramers, partially form the intermolecular bityrosine (Puchala and Schuessler, 1993). The formation of these polymer networks intermediates could diminish the mobility of the intermediates and reduce the access of the BSA to the TiO_2 electrode surface for the PC degradation reaction in the thin-layer cell. It is also possible that these large size intermediates are difficult to be further oxidized, leading to the inhibition of the catalyst surface, terminating or reducing the PC processes. The same phenomena was also observed during the photocatalytic inactivation of bacteria although the bacteria can be photocatalytically decomposed into some large molecule biological compounds. But the photocatalytic activity of catalysts can be easily found to be decrease fast with increase recycling times due to the block of the organic debris of decomposed bacteria (Shi et al., 2014).

Additionally, it is also considered that the formations of •OH could potentially lead to the change of the pH values around the microenvironment of BSA molecules, which can badly weaken the inner hydrogen bonds of BSA molecules. Therefore, the disappearance of disulfide and hydrogen bonds that are the major attributors to maintain the secondary structures of BSA molecules, which

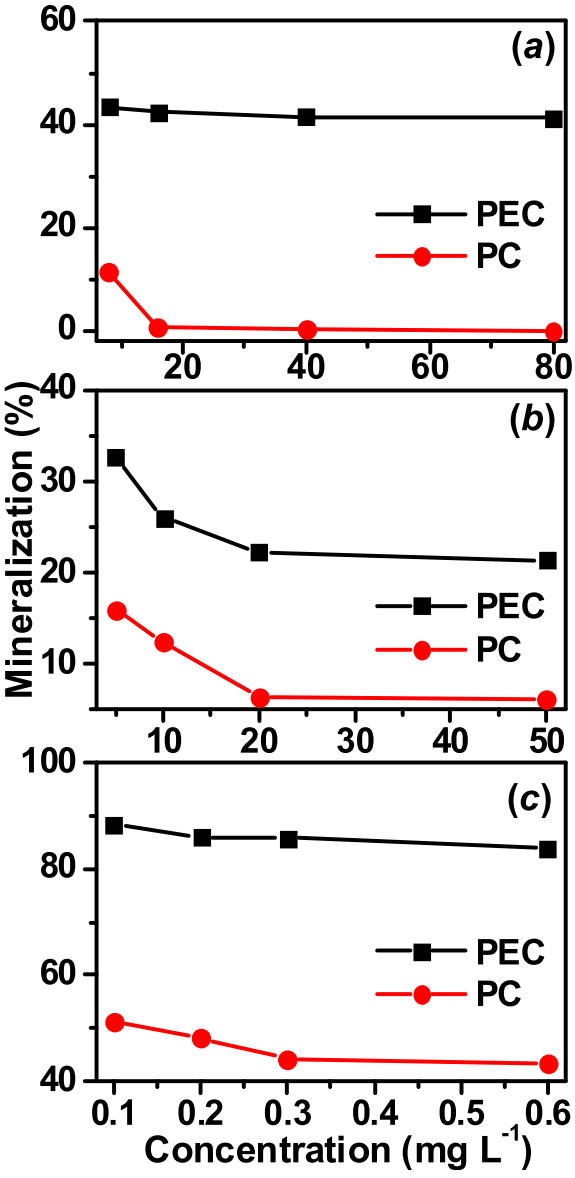

Fig. 3. PC and PEC degradation of (a) BSA; (b) lecithin; and (c) DNA.

cloud lead to the extension of the peptide chain (Wang et al., 2006). Subsequently, the remaining amino acid may spread or adhere onto the surface of TiO_2 electrode (Park et al., 2008), causing diminution of specific surface of catalyst accessible to light and the reactant. Another reason is that amino acid side chains are very important sites for oxidation agents attack at proteins due to the steric hindrance of main chain α-carbon (Hawkins and Davies, 2001). BSA is characterized by a low content of tryptophan and methionine, and a high content of cystine and the charged amino acids such as aspartic acid, glutamic acids, lysine and arginine. However, other research showed that the amino acids containing −OH (Ser), −NH (Trp, His), or−NH_2 (Asn) in their side chain appeared to be adsorbed more favorably towards photoanode and become more vulnerable to the PC oxidation and showed high decomposition rates (Tran et al., 2006).

To improve the degradation efficiencies, PEC treatment method was then applied in this study. The PEC oxidation was firstly investigated in the absence of organics. All experiments were carried out using the thin-layer photoelectrochemical cell. Compared with PC oxidation, the PEC degradation efficiencies are significantly enhanced to nearly 4 times of the degradation efficiency for PC treatment at low BSA concentration of 8 mg L^{-1} (Fig. 3a). In strong contrast to PC degradation, the PEC mineralization percentage only decreased very slightly and no decomposition termination was observed when the initial BSA concentration was further increased. Such a performance enhancement can be attributed to the combined effect of electrochemical technique and PC oxidation process. Introduction of electrochemical technique allows the application of a potential bias, which can serve as an external motive force to timely remove the photogenerated e^- from the conduction band. It is effectively suppressing the recombination of photocatalytically generated electrons/holes and leading to a dramatically improved the light efficiency (Zhao et al., 2004; Zhang et al., 2006). The ability to timely remove the photogenerated e^- from the conduction band also prolongs the lifespan of photogenrated holes, enabling the hole to directly react with BAS. The strong oxidative power of the hole (+3.1 V), which is more powerful oxidizing agent than •OH (which is the main oxidizing agent in PC process), could rapidly decompose the BSA and produced intermediates with direct contact towards the photoanode surface. Additionally, the reaction mechanisms/pathways of PC (dominated by •OH attacks) and PEC (dominated by h^+ attacks with assistance of •OH attacks) processes enhance the produced intermediates during PC and PEC processes could be different (Zhao et al., 2014; Li et al., 2015a, 2015b). These mechanistic differences between PC and PEC processes could be the essential attributors to the dramatically improved PEC performance.

3.3.2. PC and PEC degradation of L-α-lecithin

It is well known that lipids are large molecule biological compounds, possessing very different chemical compositions and properties to other large molecule biological compounds such as proteins and DNA. They are also an important class of biological compounds serving as the building bock for various microorganisms (Yin et al., 2011; Jacobson et al., 2015). To obtain evidence for better understanding the mechanistic pathways of PC and PEC decomposition of cell membranes and shed light on the need of mimicking the environment in which the TiO_2 particles will reside, lecithin was used as a model lipid in this work. This is because lecithin is not only one of the essential components of the cell membranes (Stubiger et al., 2009), but also has been widely used as a biosurfactant in the cosmetic industry for few decades (Zhao et al., 2008).

Fig. 3b shows the PC and PEC mineralization percentage of L-α-lecithin. In case of BSA degradation, the effect of the concentrations on PC mineralization percentage trend differed remarkably from the mineralization percentage trend of the PEC process, as demonstrated in Fig. 3a. In strong contrast, for the degradation of lecithin, the effect of the concentration on the mineralization percentage trend for PC and PEC processes were found to be very similar, except higher degradation efficiencies were obtained from PEC treated samples. The obtained trend of mineralization percentages decreased gradually with the increased lecithin concentration ranged from 5 to 20 mg L^{-1}. No obvious further decrease in the mineralization percentage was observed when the concentrations were greater than 50 mg L^{-1}. Though the obtained mineralization percentages of PEC were higher than those of PC within the entire concentration range investigated, the magnitude of the enhancement was not as dramatically as achieved for the case of BSA degradation. This could be due to that lecithin is a kind of lipid, in aqueous solution, its phospholipids can spontaneously form either vesicles, liposomes, bilayer sheets, micelles, or lamellar structures, depending on hydration and temperature (Bangham and Horne, 1964). A new lecithin liposome might form after the damage take place on the old lecithin liposome by PC and PEC

treatment, because of its fluid property.

3.3.3. PC and PEC degradation of DNA

Unlike lipids and proteins which are all constituents of the cell surface, the nucleic acids are located in the center of cells and are shielded against the attack by oxidants. Therefore, the shielded nucleus will be attacked after the destruction of the cell membrane, if a whole cell was subjected to PC and PEC treatment. This reaction can occur when either the nucleic acids flow out of the cell or the reactive oxygen species diffuse into the cell and initiate the oxidation of nucleic acids and other intracellular macromolecules (Sun et al., 2014). That is why very low concentration of the DNA was selected in this work as compared with that of other two large molecule biological compounds for example BSA and L-α-lecithin. It is therefore intended to investigate the PC and PEC degradation properties of *E. coli* genomic DNA.

Fig. 3c shows the PC and PEC degradation efficiencies of DNA. It revealed that 51.4% and 88.2% of 0.1 mg L^{-1} DNA were completely mineralized in the PC and PEC, respectively. That is, carbon atoms were converted to CO_2, hydrogen to H_2O and nitrogen to NH_3. The degradation efficiencies of both PC and PEC gradually decreased as the DNA concentration increased. However, the PEC degradation efficiencies curve decreased much flatter than those of PC degradation with the increase of concentration. In addition, it is worth noting that, as expected, the PC degradation ability is profoundly enhanced because the recombination of photogenerated electrons/holes can be suppressed by applied potential bias in PEC system (Zhang et al., 2006).

3.3.4. Comparison of PC and PEC degradation of large molecule biological compounds

From the above results, it was found that the degradation efficiencies of three different kinds of the biological building blocks of microorganisms can vary even at identical experimental conditions because of their unique prosperities.

Fig. 4 shows the plot of $Q_{mineralization}$ obtained from PC degradation against the Q_{COD} obtained from chemical degradation under standard COD conditions for BSA, lecithin and DNA. In case of BAS (Fig. 4a), as the initial BSA concentration increased, the $Q_{mineralization}$ decreased when plotted against the Q_{COD}, suggesting a higher mineralization efficiency of dichromate method towards BSA. The nonlinear relationship can be attributed to the inability of PC degradation of BSA as demonstrated in Fig. 3a.

In contrast, a good linearity with R^2 value of 0.9808 and 0.9996 were obtained from PC degradation of lecithin and DNA, respectively (Fig. 4b and c). The slope values of 0.046 for lecithin and 0.420 for DNA were obtained, suggesting the measured $Q_{mineralization}$ values were of 4.6% and 42% of the measured Q_{COD} values for lecithin and DNA samples, respectively. Assuming the obtained Q_{COD} values are the measure of the theoretical charge required for complete mineralization, then these results demonstrated that using Q_{COD} values as the reference, the mineralization efficiencies of 4.6% for lecithin and 42.0% for DNA were achieved under PC degradation conditions.

Fig. 5 shows the plot of $Q_{mineralization}$ obtained from PEC degradation against the Q_{COD} obtained from chemical degradation under standard COD conditions for BSA, lecithin and DNA. As seen, the good relationships with R^2 values of 1.0 for BSA, 0.9995 for lecithin and 0.9999 for DNA were obtained. These excellent linear relationships suggest that under PEC degradation conditions, the background charge generated from the water oxidation is fixed regardless of type of substrates and their concentrations.

Slope values obtained under such PEC degradation conditions were of 0.410, 0.198 and 0.831 for BSA, lecithin and DNA, respectively. If the measured Q_{COD} values are the measure of the

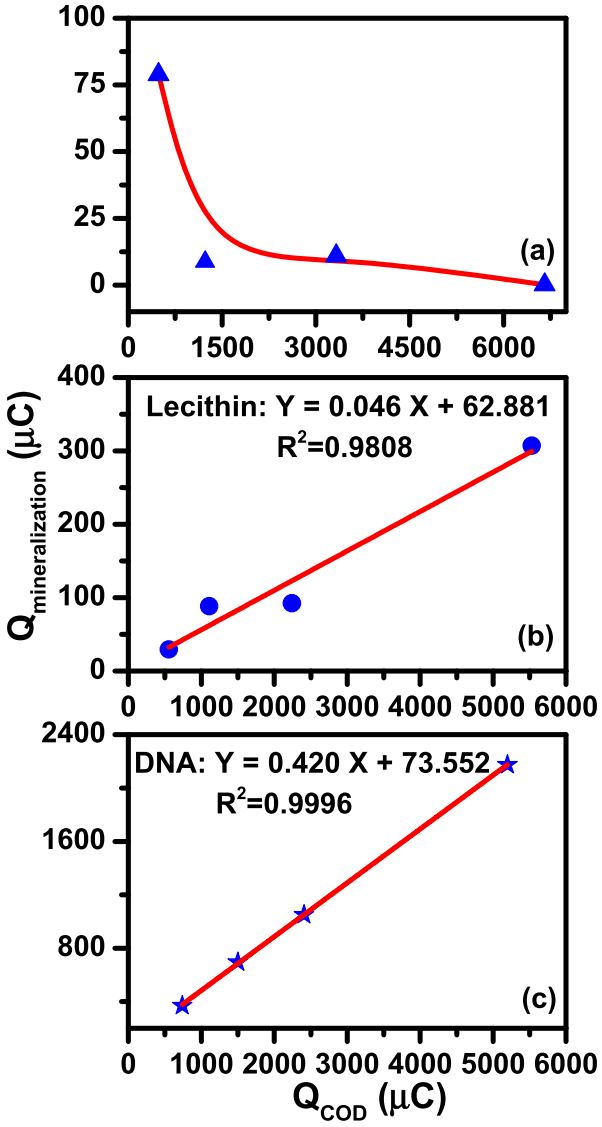

Fig. 4. Mineralization charges obtained versus initial chemical charges of (a) BSA, (b) lecithin and (c) DNA during PC degradation.

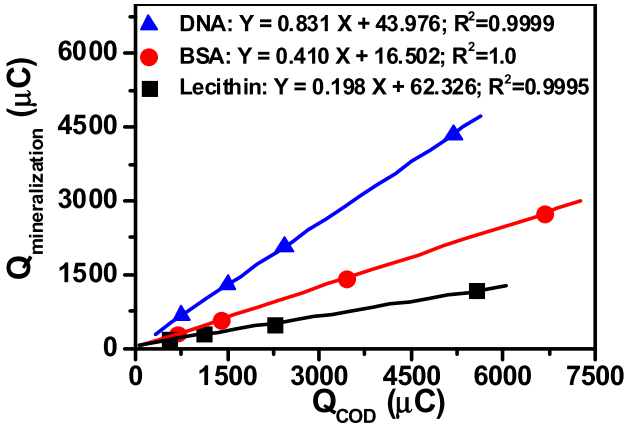

Fig. 5. Mineralized charges obtained versus initial chemical charges of BSA, lecithin and DNA during PEC degradation.

theoretical charge required for the complete mineralization, then these results demonstrated that using the Q_{COD} values as the reference, the mineralization efficiencies of 41.0% of BSA, 19.8% of lecithin and 83.1% of DNA can be achieved under PEC degradation conditions, which is much higher than those of PC mineralization efficiencies. These reveal that DNA is the easiest one to be PEC decomposed, while lecithin is the most difficult one to be decomposed among the three different types of biological compounds, under identical experimental conditions. A possible reason for high PEC degradation efficiencies of DNA could be due to its molecular structure. Chemically, DNA consists of two long polymers of simple units called nucleotides, with backbones made of sugars and phosphate groups joined by ester bonds. Two nucleotides binding together by hydrogen bonds, which can be broken relatively easily (Clausen-Schaumann et al., 2000). As previously explained, low PEC degradation efficiencies of lecithin could be also due to its unique molecular structures as some difficult oxidizable intermediates such as malondialdehyde, 4-hydroxynonenal, and lipophilic aldehydes can be produced during this process (Blake et al., 1987), although lipid is particularly susceptible to the oxidative damage (Massa et al., 2012).

4. Conclusions

As a part of the developed "bottom-up" strategy, PC and PEC degradation of large molecule biological compounds such as BSA, lecithin and bacterial genomic DNA have been quantitatively performed. To estimate the mineralization of efficiencies of these large molecule biological compounds with unknown chemical formula, a new method has been firstly developed and experimentally validated. For all large molecule biological compounds investigated are found to be PC and PEC degradable, and incomplete PC mineralization has been observed for all large molecule biological compounds investigated, especially for BSA. Furthermore, the PEC degradation method is more effective than that of PC degradation for all large molecule biological compounds investigated. And the PEC mineralization efficiency of DNA is the highest among lecithin and BSA, while the lowest PEC mineralization efficiency is obtained for lecithin. The PEC/PC mineralization ratios are found to follow an order of BSA > lecithin > DNA. This built fundamental research will provide quantitative information for further evaluation of PC and PEC destruction of microbiological pollutants with unknown chemical formulas such as bacteria and virus.

Acknowledgments

The authors thank finically support by National Natural Science Funds for Distinguished Young Scholars (41425015), National Nature Science Foundation of China (41573086 and U1201234) and Australian Research Council (ARC) Discovery Project.

Appendix A. Supplementary data

Supplementary data related to this article can be found at http://dx.doi.org/10.1016/j.watres.2016.02.066.

References

Bangham, A.D., Horne, R.W., 1964. Negative staining of phospholipids + their structural modification by-surface active agents as observed in electron microscope. J. Mol. Biol. 8, 660–668.
Blake, D.R., Allen, R.E., Lunec, J., 1987. Free-radicals in biological-systems – a review orientated to inflammatory processes. Brit. Med. Bull. 43, 371–385.
Bond, T., Templeton, M.R., Mokhtar Kamal, N.H., Graham, N., Kanda, R., 2015. Nitrogenous disinfection byproducts in English drinking water supply systems: occurrence, bromine substitution and correlation analysis. Water Res. 85, 85–94.
Bosshard, F., Riedel, K., Schneider, T., Geiser, C., Bucheli, M., Egli, T., 2010. Protein oxidation and aggregation in UVA-irradiated Escherichia coli cells as signs of accelerated cellular senescence. Environ. Microbiol. 12, 2931–2945.
Brown, J.R., 1975. Structure of bovine serum-albumin. Fed. Proc. 34, 591–591.
Cadet, J., Wagner, J.R., 2013. DNA base damage by reactive oxygen species, oxidizing agents, and UV radiation. Cold Spring Harb. Perspect. Biol. 5 http://dx.doi.org/10.1101/cshperspect.a012559.
Chuang, Y.H., Lin, A.Y.C., Wang, X.H., Tung, H.H., 2013. The contribution of dissolved organic nitrogen and chloramines to nitrogenous disinfection byproduct formation from natural organic matter. Water Res. 47, 1308–1316.
Clausen-Schaumann, H., Rief, M., Tolksdorf, C., Gaub, H.E., 2000. Mechanical stability of single DNA molecules. Biophys. J. 78, 1997–2007.
Dalrymple, O.K., Isaacs, W., Stefanakos, E., Trotz, M.A., Goswami, D.Y., 2011. Lipid vesicles as model membranes in photocatalytic disinfection studies. J. Photochem. Photobiol. A Chem. 221, 64–70.
Dean, R.T., Fu, S.L., Stocker, R., Davies, M.J., 1997. Biochemistry and pathology of radical-mediated protein oxidation. Biochem. J. 324, 1–18.
Hawkins, C.L., Davies, M.J., 2001. Generation and propagation of radical reactions on proteins. Biochim. Biophys. Acta Bioenerg. 1504, 196–219.
Hirayama, K., Akashi, S., Furuya, M., Fukuhara, K., 1990. Rapid confirmation and revision of the primary structure of bovine serum-albumin by ESIMS and Frit-FAB LC/MS. Biochem. Biophys. Res. Co. 173, 639–646.
Jacobson, K.H., Gunsolus, I.L., Kuech, T.R., Troiano, J.M., Melby, E.S., Lohse, S.E., Hu, D., Chrisler, W.B., Murphy, C.J., Orr, G., Geiger, F.M., Haynes, C.L., Pedersen, J.A., 2015. Lipopolysaccharide density and structure govern the extent and distance of nanoparticle interaction with actual and model bacterial outer membranes. Environ. Sci. Technol. 49, 10642–10650.
Ji, Y.F., Ferronato, C., Salvador, A., Yang, X., Chovelon, J.M., 2014. Degradation of ciprofloxacin and sulfamethoxazole by ferrous-activated persulfate: implications for remediation of groundwater contaminated by antibiotics. Sci. Total Environ. 472, 800–808.
Kurz, J., Eberle, F., Graumann, T., Kaschel, M.E., Sahr, A., Neumann, F., Dalpke, A.H., Erdinger, L., 2011. Inactivation of LPS and RNase A on photocatalytically active surfaces. Chemosphere 84, 1188–1193.
Li, G.Y., Liu, X.L., An, J.B., Yang, H., Zhang, S.Q., Wong, P.K., An, T.C., Zhao, H.J., 2015a. Photocatalytic and photoelectrocatalytic degradation and mineralization of small biological compounds amino acids at TiO_2 photoanodes. Catal. Today 245, 46–53.
Li, G.Y., Liu, X.L., An, T.C., Yang, H., Zhang, S.Q., Zhao, H.J., 2015b. Photocatalytic and photoelectrocatalytic degradation of small biological compounds at TiO_2 photoanode: a case study of nucleotide bases. Catal. Today 242 (Part B), 363–371.
Li, G.Y., Liu, X.L., Zhang, H.M., Wong, P.K., An, T.C., Zhao, H.J., 2013a. Comparative studies of photocatalytic and photoelectrocatalytic inactivation of *E. coli* in presence of halides. Appl. Catal. B Environ. 140–141, 225–232.
Li, G.Y., Liu, X.L., Zhang, H.M., Wong, P.K., An, T.C., Zhou, W.Q., Li, B., Zhao, H.J., 2014. Adenovirus inactivation by in situ photocatalytically and photoelectrocatalytically generated halogen viricides. Chem. Eng. J. 253, 538–543.
Li, G.Y., Zhang, Y.L., Sun, H.W., An, J.B., Nie, X., Zhao, H.J., Wong, P.K., An, T.C., 2013b. Photocatalytic and photoelectrocatalytic degradation of small biological compounds: a case study of uridine. Catal. Today 201, 167–174.
Li, G.Y., Liu, X.L., Zhang, H.M., An, T.C., Zhang, S.Q., Carroll, A.R., Zhao, H.J., 2011. In situ photoelectrocatalytic generation of bactericide for instant inactivation and rapid decomposition of Gram-negative bacteria. J. Catal. 277, 88–94.
Martinez, J.L., 2008. Antibiotics and antibiotic resistance genes in natural environments. Science 321, 365–367.
Massa, A., Vione, D., Ugazio, E., Gastaldi, L.E., Carlotti, M.E., 2012. Effect of reactive species photogenerated by the ultraviolet irradiation of TiO_2 on the peroxidation of linoleic acid. J. Dispers. Sci. Technol. 33, 1615–1620.
Nie, X., Li, G.Y., Gao, M.H., Sun, H.W., Liu, X.L., Zhao, H.J., Wong, P.K., An, T.C., 2014. Comparative study on the photoelectrocatalytic inactivation of *Escherichia coli* K-12 and its mutant *Escherichia coli* BW25113 using TiO2 nanotubes as a photoanode. Appl. Catal. B Environ. 147, 562–570.
Nowicka, A.M., Kowalczyk, A., Sek, S., Stojek, Z., 2013. Oxidation of DNA followed by conformational change after OH radical attack. Anal. Chem. 85, 355–361.
Park, S.J., Kim, N.H., Jeong, B.H., Jin, J.K., Choi, J.K., Park, Y.J., Kim, J.I., Carp, R.I., Kim, Y.S., 2008. The effect of Fenton reaction on protease-resistant prion protein (PrPSc) degradation and scrapie infectivity. Brain Res. 1238, 172–180.
Paspaltsis, I., Berberidou, C., Poulios, I., Sklaviadis, T., 2009. Photocatalytic degradation of prions using the photo-Fenton reagent. J. Hosp. Infect. 71, 149–156.
Puchala, M., Schuessler, H., 1993. Oxygen effect in the radiolysis of proteins .3. hemoglobin. Int. J. Radiat. Biol. 64, 149–156.
Sambrook, J., Fritsch, E.F., Maniatis, T., 1989. Molecular Cloning: a Laboratory Manual, second ed. ed. Cold Spring Harbor Laboratory, Cold Spring Harbor, New York.
Sharma, K.K.K., Swarts, S.G., Bernhard, W.A., 2011. Mechanisms of direct radiation damage to DNA: the effect of base sequence on base end products. J. Phys. Chem. B 115, 4843–4855.
Shi, H.X., Li, G.Y., Sun, H.W., An, T.C., Zhao, H.J., Wong, P.K., 2014. Visible-light-driven photocatalytic inactivation of E. coli byAg/AgX-CNTs (X = Cl, Br, I) plasmonic photocatalysts: bacterialperformance and deactivation mechanism. Appl. Catal. B Environ. 158–159, 301–307.
Stubiger, G., Pittenauer, E., Belgacem, O., Rehulka, P., Widhalm, K., Allmaier, G., 2009. Analysis of human plasma lipids and soybean lecithin by means of high-performance thin-layer chromatography and matrix-assisted laser desorption/ionization mass spectrometry. Rapid Commun. Mass Spectrom. 23, 2711–2723.

Sun, H.W., Li, G.Y., Nie, X., Shi, H.X., Wong, P.K., Zhao, H.J., An, T.C., 2014. Systematic approach to in-depth understanding of photoelectrocatalytic bacterial inactivation mechanisms by tracking the decomposed building blocks. Environ. Sci. Technol. 48, 9412–9419.

Tobaldi, D.M., Piccirillo, C., Pullar, R.C., Gualtieri, A.F., Seabra, M.P., Castro, P.M.L., Labrincha, J.A., 2014. Silver-modified nano-titania as an antibacterial agent and photocatalyst. J. Phys. Chem. C 118, 4751–4766.

Tran, T.H., Nosaka, A.Y., Nosaka, Y., 2006. Adsorption and photocatalytic decomposition of amino acids in TiO_2 photocatalytic systems. J. Phys. Chem. B 110, 25525–25531.

Wang, J., Ding, N., Zhang, Z.H., Wang, S.X., Guo, Y., Liu, B., Zhang, Y.Y., Zhang, X.D., 2009. Sonocatalytic damage of bovine serum albumin (BSA) under ultrasonic irradiation by mixed TiO_2/SiO_2 powder. J. Chem. Technol. Biotechnol. 84, 538–546.

Wang, J., Wu, J., Zhang, Z.H., Zhang, X.D., Pan, Z.J., Wang, L., Xu, L.A., 2006. Sonocatalytic damage of bovine serum albumin (BSA) in the presence of nanometer anatase titanium dioxide (TiO_2). Ultrasound Med. Biol. 32, 147–152.

Wang, X.N., Li, G.S., Zhu, H.J., Yu, J.C., Xiao, X.D., Li, Q., 2014. Vertically aligned CdTe nanotube arrays on indium tin oxide for visible-light-driven photoelectrocatalysis. Appl. Catal. B Environ. 147, 17–21.

Westgatet, P.J., Park, C., 2010. Evaluation of proteins and organic nitrogen in wastewater treatment effluents. Environ. Sci. Technol. 44, 5352–5357.

Xu, D., Cheng, F., Lu, Q., Dai, P., 2014. Microwave enhanced catalytic degradation of methyl orange in aqueous solution over CuO/CeO_2 catalyst in the absence and presence of H_2O_2. Ind. Eng. Chem. Res. 53, 2625–2632.

Yin, H., Xu, L., Porter, N.A., 2011. Free radical lipid peroxidation: mechanisms and analysis. Chem. Rev. 111, 5944–5972.

Zeleny, T., Ruckenbauer, M., Aquino, A.J.A., Muller, T., Lankas, F., Drsata, T., Hase, W.L., Nachtigallova, D., Lischka, H., 2012. Strikingly different effects of hydrogen bonding on the photodynamics of individual nucleobases in DNA: comparison of guanine and cytosine. J. Am. Chem. Soc. 134, 13662–13669.

Zhang, S.Q., Jiang, D.L., Zhao, H.J., 2006. Development of chemical oxygen demand on-line monitoring system based on a photoelectrochemical degradation principle. Environ. Sci. Technol. 40, 2363–2368.

Zhang, S.Q., Zhao, H.J., Jiang, D.L., John, R., 2004. Photoelectrochemical determination of chemical oxygen demand based on an exhaustive degradation model in a thin-layer cell. Anal. Chim. Acta 514, 89–97.

Zhao, H.J., Jiang, D.L., Zhang, S.Q., Catterall, K., John, R., 2004. Development of a direct photoelectrochemical method for determination of chemical oxygen demand. Anal. Chem. 76, 155–160.

Zhao, H.J., Jiang, D.L., Zhang, S.L., Wen, W., 2007. Photoelectrocatalytic oxidation of organic compounds at nanoporous TiO_2 electrodes in a thin-layer photoelectrochemical cell. J. Catal. 250, 102–109.

Zhao, S.L., Yin, H.J., Du, L., He, L.C., Zhao, K., Chang, L., Yin, G.P., Zhao, H.J., Liu, S.Q., Tang, Z.Y., 2014. Carbonized nanoscale metal-organic frameworks as high performance electrocatalyst for oxygen reduction reaction. ACS Nano 8, 12660–12668.

Zhao, Y.J., Zhang, J.L., Han, B.X., Zhang, C.X., Li, W., Feng, X.Y., Hou, M.Q., Yang, G.Y., 2008. Effect of compressed CO_2 on the properties of lecithin reverse micelles. Langmuir 24, 9328–9333.